Partially disordered antiferromagnetic phase in Ca3CoRhO6

AUTHOR(S):

Niitaka, S; Yoshimura, K; Kosuge, K; Nishi, M; Kakurai, K

CITATION:

Niitaka, S ...[et al]. Partially disordered antiferromagnetic phase in Ca3CoRhO6. PHYSICAL REVIEW LETTERS 2001, 87(17): 177202.

ISSUE DATE:

2001-10-22

URL:

http://hdl.handle.net/2433/49927

Partially Disordered Antiferromagnetic Phase in Ca_3CoRhO_6

S. Niitaka,[1] K. Yoshimura,[1] K. Kosuge,[1] M. Nishi,[2] and K. Kakurai[2,3]

[1]*Department of Chemistry, Graduate School of Science, Kyoto University, Kyoto 606-8502, Japan*
[2]*Neutron Scattering Laboratory, Institute for Solid State Physics, University of Tokyo, 106-1 Shirakata, Tokai, Ibaraki, 319-1106, Japan*
[3]*Advanced Science Research Center, Japan Atomic Energy Research Institute, Tokai, Ibaraki 319-1195, Japan*
(Received 24 May 2001; published 4 October 2001)

Neutron diffraction experiments are reported on Ca_3CoRhO_6 which consists of ferromagnetic Ising spin chains on a triangular lattice. It was first confirmed from temperature dependence of the (110) peak intensity that Ca_3CoRhO_6 realizes a partially disordered antiferromagnetic state, where $2/3$ of the ferromagnetic chains order antiferromagnetically with each other and the remaining $1/3$ are left incoherent with the other chains. The $1/3$ incoherent ferromagnetic Ising chains freeze to maintain a disordered state at lower temperatures. This compound is successfully discussed as a candidate of a nonequilibrium one-dimensional Ising model.

DOI: 10.1103/PhysRevLett.87.177202 PACS numbers: 75.25.+z, 75.30.Kz

The physics of triangular lattice systems has been of much interest because geometrical spin frustration produces novel types of phase transitions. Especially, a partially disordered antiferromagnetic (PDA) state discovered by Mekata [1] in $CsCoCl_3$ has been attracting considerable attention as an exotic phase peculiar to the triangular-lattice antiferromagnet with Ising spin [2]. In $CsCoCl_3$, the linear chains consisting of Co^{2+} ions with effective spin $S = 1/2$ along the c axis form a triangular lattice in the c plane. Antiferromagnetic intrachain interactions are much stronger than antiferromagnetic interchain interactions. Consequently the magnetic chain with well-developed short-range antiferromagnetic order can be considered to behave as one Ising spin before the onset of the magnetic phase transition, exhibiting the character of the triangular lattice. $CsCoCl_3$ undergoes two successive magnetic phase transitions at $T_{N_1} = 21$ K and $T_{N_2} = 9$ K. In the temperature region between T_{N_1} and T_{N_2}, there appears the noteworthy PDA phase where $2/3$ of the magnetic chains order antiferromagnetically leaving the rest incoherent. The PDA structure projected on the c plane is illustrated in Fig. 1(a). The Monte Carlo simulation indicates the appearance of the PDA state on the above triangular network with next-nearest-neighbor (NNN) ferromagnetic interchain interactions [3]. The origin of incoherent chain formation is the cancellation of the antiferromagnetic interchain interactions with six nearest-neighbor (NN) chains and the entropy effect (TS) surpassing NNN ferromagnetic interchain interactions between incoherent chains. Spin reversal in the incoherent antiferromagnetic chains is easily induced by the propagation of a domain wall like a solitary wave (soliton) [4]. Below T_{N_2}, incoherent chains order ferromagnetically in the c plane, resulting in a ferrimagnetic (FR) state, as illustrated in Fig. 1(b). Another compound exhibiting the PDA state on a triangular lattice of antiferromagnetic Ising-spin chains is, as far as we know, only $CsCoBr_3$ [5]. Moreover, no compound exists in the case of ferromagnetic Ising-spin chains.

Ca_3CoRhO_6 dealt with in this Letter was suggested to have the PDA state with ferromagnetic Ising-spin chains on a triangular lattice [6]. Ca_3CoRhO_6 with the rhombohedral K_4CdCl_6 structure (space group $R\bar{3}c$) contains linear chains consisting of alternating face-sharing CoO_6 trigonal prisms and RhO_6 octahedra. The chains along the c axis are separated by calcium cations, forming a triangular lattice in the c plane. Therefore, Ca_3CoRhO_6 has the structural similarity with $CsCoCl_3$ in the respect that chains consisting of magnetic ions are arranged on a triangular lattice. The magnetization measurements using field-oriented powder samples indicated the positive Weiss temperature of 150 K and the strong Ising anisotropy along the c axis, suggesting that Ca_3CoRhO_6 possesses ferromagnetic Ising-spin chains. The magnetic susceptibility M/H of Ca_3CoRhO_6 exhibits two characteristic temperatures, $T_1 = 90$ K and $T_2 = 30$ K [see the inset of Fig. 2(a)]. The M/H depends on H below T_1. There is a sharp drop at T_2, reaching nearly zero in measurements after zero field cooling (ZFC), while the M/H does not

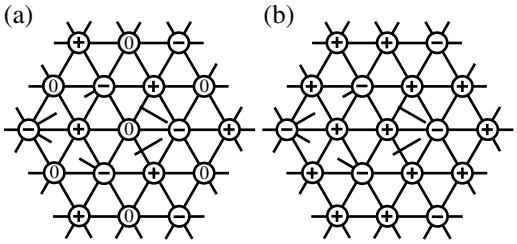

FIG. 1. Schematic illustration of (a) PDA structure and (b) FR structure projected on the c plane. The circles represent antiferromagnetic (ferromagnetic) Ising-spin chains. The plus and minus signs stand for the directions of the representative moment of the chains. The zero (0) represents spin direction as either + or − at random, i.e., the incoherent chain.

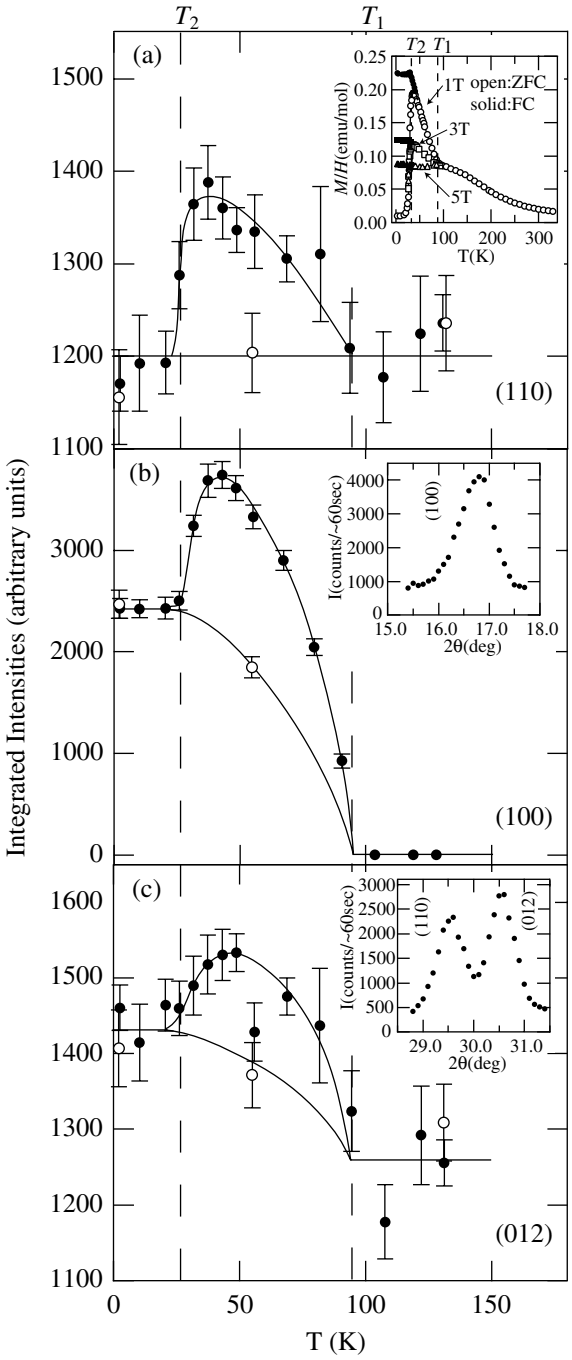

FIG. 2. Temperature dependence of the integrated intensity of (a) (110), (b) (100), and (c) (012) peaks at 0 T (○) and 2 T (●). The solid lines are guides to the eye. The inset in (a) shows the temperature dependence of M/H of Ca_3CoRhO_6 measured at $H = 1$, 3, and 5 T. The insets in (b) and (c) show the typical neutron diffraction patterns around the (100) peak and around (110) and (012) peaks at 2 K under 0 T, respectively.

drop in measurements after field cooling (FC). In the previous powder neutron diffraction experiment, four magnetic Bragg peaks with the Miller indices (100), (200), (112), and (210) based on the chemical unit cell were observed at both 4 K (below T_2) and 40 K (between T_2 and T_1). The neutron diffraction patterns at 4 K and 40 K can be explained qualitatively by both the PDA and the FR structure of ferromagnetic Ising-spin chains on a triangular lattice, as shown in Fig. 1, the latter of which possibly realizes in $Ca_3Co_2O_6$ at low temperatures [7]. Neither of these two possible models could be eliminated by Rietveld refinement because of the large error in the previous neutron diffraction experiment.

In order to elucidate the magnetic state below T_1 and the origin of the anomaly below T_2 observed in the magnetic susceptibility, we performed neutron diffraction experiments by both polarized and unpolarized neutron beams. Temperature dependences of the integrated intensities of (110), (100), and (012) peaks were measured under an applied magnetic field of 0–2 T after ZFC. It is a crucial point in determining the magnetic structure that the (110) peak does not include a magnetic component in the case of PDA, while it does include a finite magnetic component in the case of FR structure. We also checked the depolarization of polarized neutrons passing straight through the sample in order to distinguish whether the magnetic domains with spontaneous magnetization exist at low temperatures, or not. Our experimental results first indicated evidently that the PDA state with ferromagnetic Ising-spin chains appeared in Ca_3CoRhO_6. This phase is a novel magnetic phase discovered in this study for the first time, as stated above. Furthermore, the $1/3$ incoherent chains in the PDA state freeze to maintain a disordered state at lower temperatures, which indicates that the state at lower temperatures is not a thermodynamically stable state.

Neutron diffraction experiments were performed on the polarized neutron triple axis spectrometer installed at the Japan Research Reactor 3M, Japan Atomic Energy Research Institute, Tokai, Japan. An uncrushed sintered pellet (a column of 13 mm $\phi \times 39$ mm with a mass of 18.5 g) sample was used in order to prevent it from rotating by applied magnetic field. The X-ray diffraction measurement confirmed random orientation of the pelletized crystalline sample. The incident neutron wavelength was fixed at $\lambda = 2.35$ Å. The (002) reflection of pyrolytic graphite (PG) was used for both the monochromator and the analyzer. A PG filter was placed in front of the monochromator to eliminate higher-order contaminations. The horizontal collimations were open-80′-40′-open. The sample inside an aluminum can was mounted in a horizontal-field superconducting magnet. The data were collected in the 2θ ranges of 15.4°–17.7° and 28.8°–31.4° in the temperature range of 2–130 K under applied magnetic fields of 0–2 T after ZFC. The components of the (110) and (012) peaks and that of the (100) peak were derived by fitting the neutron diffraction patterns [e.g., insets of Figs. 2(b) and 2(c)] with two Gaussians and one Gaussian with the constant terms corresponding to the backgrounds, respectively. Rietan calculations were used in the structure factors of neutron diffractions [8] in order to compare experiments with models. For the depolarization check, polarized neutrons were produced and analyzed by utilizing the (111) reflection of magnetized Cu_2MnAl Heusler-alloy single crystals. The polarization

state of the neutron beam can be changed by a π-flipper device positioned before the sample. The polarization of the beam is determined by measuring the nonspin flip and spin flip intensities of polarized neutrons passing the sample with the π flipper off and on, respectively. The depolarization checks were carried out at 2 K under guide fields of 1 and 2 T after ZFC. No bulk magnetization was observed under these conditions.

In Fig. 2(a), we show the temperature dependence of the integrated intensity of the (110) peak. The intensity at 0 T, $I_{0\,\mathrm{T}}^{(110)}$, shows no increase below T_1, indicating that there exists no magnetic contribution to the (110) peak which clearly indicates that Ca_3CoRhO_6 realizes the PDA state below T_1 instead of the FR state. No magnetic component of $I_{0\,\mathrm{T}}^{(110)}$ down to 2 K also indicates no magnetic phase transition from the PDA state to the FR state, unlike $CsCoCl_3$ and $CsCoBr_3$. The intensity at 2 T, $I_{2\,\mathrm{T}}^{(110)}$, below T_2 is the same as $I_{0\,\mathrm{T}}^{(110)}$, indicating no change in the magnetic structure even by applying the magnetic field of 2 T. By taking into account, together with the above result, that the magnetic susceptibility below T_2 in ZFC measurements has a very small value different from those in FC measurements, we can consider that the Ising spins in the incoherent chains should freeze to maintain a disorder state below T_2. Therefore, we call the PDA state below T_2 a frozen PDA (F-PDA) state. $I_{2\,\mathrm{T}}^{(110)}$ sharply increases above T_2, leading to the magnetic phase transition from the F-PDA state to the field-induced FR (FIFR) state accompanied by the melting of the frozen spins, characterized by the plateau at $1/3$ of the full moment around 3 T in the magnetization curve at the temperature between T_2 and T_1 [6]. Hence T_2 can be considered as the freezing/melting point of ferromagnetic Ising-spin chains. With rising temperature above T_2, $I_{2\,\mathrm{T}}^{(110)}$ gradually reduces to the same as $I_{0\,\mathrm{T}}^{(110)}$ above T_1 of the long-range magnetic ordered temperature.

To exclude the existence of the ferrimagnetic domains and confirm the F-PDA state below T_2, we further carried out the depolarization check of polarized neutrons. This experiment is based on the principle of the depolarizer: Polarized neutrons are depolarized by passing through a magnetic material with the local spontaneous magnetizations of the domains randomly oriented. Therefore, the depolarization check is considered to be a very simple method to determine whether a magnetic structure has spontaneous magnetization, or not. The polarization of the polarized beam passing through the sample remained at 85% and 87% after ZFC at 2 K under the applied field of 1 and 2 T, respectively. This indicates that the polarization of the neutrons remains substantial and suggests the existence of the F-PDA state instead of the FR state. A FR structure with finite spontaneous magnetization randomly oriented would definitely contribute to the depolarization of the neutron beam unlike the F-PDA structure without spontaneous magnetization.

Figure 2(b) shows the temperature dependence of the integrated intensity of the (100) peak. The intensity at 0 T, $I_{0\,\mathrm{T}}^{(100)}$, has finite values below T_1 and rises with decreasing temperature between T_2 and T_1. Below T_2, $I_{0\,\mathrm{T}}^{(100)}$ shows no increase, indicating that the spin freezing realizes below T_2. The behavior of the intensity at 2 T, $I_{2\,\mathrm{T}}^{(100)}$, can be interpreted as the same as the case with $I_{2\,\mathrm{T}}^{(110)}$. We roughly estimated magnetic components of the PDA state and the FIFR state for the (100) peak, $|F_{\mathrm{PDA}}^{(100)}|^2$ and $|F_{\mathrm{FIFR}}^{(100)}|^2$, as follows. For the PDA state, It was extrapolated with $T \rightarrow T_2$ from higher temperature region using $I_{0\,\mathrm{T}}^{(100)}$ and for the FIFR state, extrapolated similarly using $I_{2\,\mathrm{T}}^{(100)}$. Thus, the experimentally estimated values of $|F_{\mathrm{PDA}}^{(100)}|^2$ and $|F_{\mathrm{FIFR}}^{(100)}|^2$ were 2430 and 4000, respectively, giving the ratio of $|F_{\mathrm{FIFR}}^{(100)}|^2/|F_{\mathrm{PDA}}^{(100)}|^2$ as 1.65. The calculated ratio by Rietan is 1.33 independent of the moments of Co and Rh, which roughly agrees with the experimental ratio but is a little smaller. It suggests the occurrence of the switching between the three sublattices of the PDA structure. A frequent switching is indeed observed in the Monte Carlo simulation [9].

We also estimated the magnetic parts of the (110) and (012) peaks. For each peak, the magnetic parts in the PDA and the FIFR state were estimated by subtracting the value above T_1 corresponding to the nuclear part from the values extrapolated in the same way as the case with the (100) peak. The experimental ratios of $|F_{\mathrm{PDA}}^{(012)}|^2/|F_{\mathrm{FIFR}}^{(110)}|^2$ and $|F_{\mathrm{FIFR}}^{(012)}|^2/|F_{\mathrm{FIFR}}^{(110)}|^2$ were 0.85 and 1.5, respectively. We calculated the magnetic components for the following two cases to compare with the experimental ratios. First, the Co ions are in the trivalent state with the magnetic moment of $4\mu_B$ and the Rh ions are in the trivalent state with $0\mu_B$. Second, the Co ions are in the divalent state with $3\mu_B$ and the Rh ions are in the tetravalent state with $1\mu_B$. Both cases are based on the experimental facts of the saturation magnetization being $4\mu_B$ in the magnetization curves and the total valence of Co and Rh being 6. The calculated ratios of $|F_{\mathrm{PDA}}^{(012)}|^2/|F_{\mathrm{FIFR}}^{(110)}|^2$ and $|F_{\mathrm{FIFR}}^{(012)}|^2/|F_{\mathrm{FIFR}}^{(110)}|^2$ for the former case are 0.86 and 1.4, and for the latter case are 0.29 and 0.49. The experimental ratios agree well with the former, while there is a large deviation from the latter. It suggests that the valences of Co and Rh are trivalent, and that the spin configuration of Ca_3CoRhO_6 is the same as that of $Ca_3Co_2O_6$ in which alternating trigonal prismatic and octahedral coordinated cobalt ions are in the trivalent state with $4\mu_B$ (high spin) and $0\mu_B$ (low spin), respectively, because of the difference in the strength of their crystalline fields [7].

The backgrounds of the (100) peak and that of the (110) and (012) peaks under 2 T after ZFC, which correspond to the constant terms in the fittings of the diffraction peaks as mentioned above, show a peculiar temperature dependence, as seen in Fig. 3. The backgrounds at 0 T increase monotonously with rising temperature to T_1. The backgrounds under 2 T, however, show a sharp drop at T_2

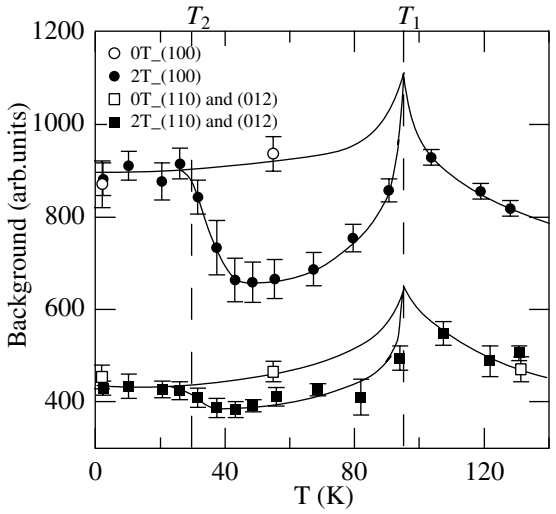

FIG. 3. Temperature dependence of the background intensity of the (100) peak at 0 T (○) and 2 T (●) and the (110) and (012) peaks at 0 T (□) and 2 T (■). The solid lines are guides to the eye.

anomalously and then increase towards T_1, indicating that the backgrounds are affected by the quasielastic critical neutron scattering characteristic of a magnetic phase transition. Above T_1, they again decrease. The key to the anomalous sharp drops at T_2 is the diffuse scattering of the $1/3$ incoherent ferromagnetic Ising-spin chains. The irregular drop at T_2 can be explained as follows. Below T_2 after ZFC, the $1/3$ incoherent ferromagnetic Ising-spin chains cause diffuse scatterings around the (100), (110), and (012) peaks. The diffuse scatterings are included in the constant terms in the fittings of the diffraction peaks. Hence the backgrounds below T_2 increase by the diffuse scatterings. The field-induced transition from the F-PDA to the FR state at T_2 changes the diffuse scatterings of the $1/3$ incoherent chains to the magnetic parts of the diffraction peaks due to their ferromagnetic long-range order. Consequently the backgrounds decrease while the integrated intensities of the (110), (100), and (012) peaks under 2 T increase, as seen in Figs. 2 and 3. It is interesting that the picture of the diffuse scattering due to the incoherent chains manifests in the estimated backgrounds.

Finally we discuss the PDA state in Ca_3CoRhO_6 briefly. It is worth noting that $Ca_3Co_2O_6$ does not exhibit the PDA state, unlike Ca_3CoRhO_6, although they have the same triangular spin arrangement. It can be considered as the reason that replacing octahedral coordinated cobalt ions by rhodium ions changes the relationship between the NN antiferromagnetic interchain interactions and the NNN ferromagnetic interchain interactions, inducing the stability of the PDA state from the viewpoint of a magnetic free energy diagram. It is also likely that spin inversions in the incoherent ferromagnetic chains are caused by the propagation of the domain walls. The most important point of the PDA state in Ca_3CoRhO_6 is that the state at lower temperatures is not the FR state but the F-PDA state, in contrast to $CsCoCl_3$. We think that it originates from the difference in the process of the propagation of the domain walls between the antiferromagnetic and ferromagnetic chains based on the theoretical studies [10]. In the antiferromagnetic chains, the domain walls can propagate with small transverse exchange interactions. On the other hand, they cannot produce the propagation of the domain walls in the ferromagnetic chains. Hence the domain walls in the ferromagnetic chains can propagate only by a thermally activated process which becomes extremely slow at low temperatures. Given that the essential freezing of the propagation of the domain walls occurs above the temperature below which the FR state is a thermodynamically stable state, we can explain the appearance of the F-PDA state which is not a thermodynamically stable state but is produced by quenching from the PDA state. It shows that Ca_3CoRhO_6 is useful for studying a nonequilibrium one-dimensional Ising-spin system.

In conclusion, the neutron diffraction experiments on Ca_3CoRhO_6 have confirmed, for the first time, that the PDA structure is realized on a triangular lattice made up of ferromagnetic Ising-spin chains. We propose that the F-PDA state at lowest temperatures can be a good model of a nonequilibrium one-dimensional Ising-spin system which will contribute greatly to the study of nonequilibrium critical phenomena.

We thank H. Kageyama and M. Kato for useful discussions. This study was supported by a Grant-in-Aid on priority area, "Novel Quantum phenomena in Transition Metal Oxides," from the Ministry of Education, Science, Sports and Culture, and also partially supported by a Grant-in-Aid for Scientific Research of the Japan Society for the Promotion of Science (11440195, 12440195, 12874038).

[1] M. Mekata, J. Phys. Soc. Jpn. **42**, 76 (1977).
[2] See, for example, T. Kohmoto *et al.,* Phys. Rev. B **57**, 2936 (1998), and references therein.
[3] O. Koseki and F. Matsubara, J. Phys. Soc. Jpn. **69**, 1202 (2000).
[4] K. Adachi, J. Phys. Soc. Jpn. **50**, 3904 (1981).
[5] W. B. Yelon, D. E. Cox, and M. Eibschütz, Phys. Rev. B **12**, 5007 (1975).
[6] S. Niitaka *et al.,* J. Solid State Chem. **146**, 137 (1999); S. Niitaka *et al.,* J. Phys. Soc. Jpn. **70**, 1222 (2001).
[7] S. Aasland, H. Fjellvåg, and B. Hauback, Solid State Commun. **101**, 187 (1997); H. Kageyama *et al.,* J. Phys. Soc. Jpn. **67**, 357 (1998).
[8] F. Izumi, in *The Rietveld Method,* edited by R. A. Young (Oxford University Press, Oxford, 1993), Chap. 13.
[9] S. Fujiki *et al.,* J. Phys. Soc. Jpn. **52**, 1531 (1983).
[10] J. Villain, Physica (Amsterdam) **79B**, 1 (1975); N. Ishikawa and H. Shiba, Prog. Theor. Phys. **63**, 743 (1980).